Parallel two-channel near- and far-field fluorescence microscopy

Dorinel Verdes
Thomas Ruckstuhl
Stefan Seeger
Universität Zürich
Physikalisch-Chemisches Institut
Winterthurerstrasse 190
Zürich CH-8057, Switzerland
E-mail: sseeger@pci.unizh.ch

Abstract. We report a new two-channel fluorescence microscopy technique for surface-generated fluorescence. The realized fluorescence microscope allows high resolution imaging of aqueous samples. The core element of the instrument is a parabolic mirror objective that is used to collect the fluorescence at large surface angles above the critical angle of the water/glass interface. An aspheric lens, incorporated into the solid parabolic element, is used for diffraction-limited laser focusing and for collecting fluorescence at low angles with respect to the optical axis. By separated collection of the fluorescence emitted into supercritical and subcritical angles, two detection volumes strongly differing in their axial resolution are generated at the surface of a glass cover slip. The collection of supercritical angle fluorescence (SAF) results in a strict surface confinement of the detection volume, whereas collecting below the critical angle allows gathering the fluorescence emitted several microns deep inside the sample. Consequently, the signals from surface-bound and unbound diffusing fluorescent molecules can be obtained simultaneously. [DOI: 10.1117/1.2747627]

Keywords: geometrical optics; optical design; fluorescence microscopy; confocal microscopy; total internal reflection.

Paper 06301 received Oct. 27, 2006; accepted for publication Feb. 20, 2007; published online Jun. 15, 2007.

1 Introduction

Fluorescence microscopy is one approach for single molecule detection (SMD) and is particularly suitable to obtain information about dynamic processes with high spectral and temporal resolution.[1,2] Confocal optics is a widely used technique for SMD due to its excellent signal-to-background ratio and the high count rate obtainable per molecule. A well-established confocal method to study biomolecular interactions in solution is fluorescence correlation spectroscopy (FCS).[3] However, many bioanalytical applications, such as heterogeneous immunoassays,[4] DNA assays,[5] and cell experiments[6] on solid substrates, involve fluorescence detection in close proximity to interfaces.

On this account, total internal reflection fluorescence (TIRF) microscopy has been established for investigating surface fluorescence with negligible background interference from unbound, freely diffusing molecules in solution.[6,7] In this technique, the illumination above the critical angle produces an evanescent excitation field that extends into the sample volume between one to several hundred nanometers. Fluorescence imaging at interfaces has been achieved using prism-type[8–11] and objective-type TIRF microscopy.[11–14] The latter is often preferred because of its higher fluorescence collection efficiency and it is more user friendly.

Focusing the light beam above the critical angle of a high numerical aperture objective (>1.4) does, however, present some technical difficulties.[15,16] One impediment for combining TIRF excitation with confocal optics is that microscope objectives of high numerical apertures do not usually perform submicron focusing of the illumination at the surface incident at supercritical angles.[14–16] As a consequence, the illumination of a large surface area can be unfavorable for some applications because it can increase the photobleaching processes substantially.[15] To improve the focus at the glass/water interface for the objective-type TIRF excitation, an annulus illumination has been used.[17,18] Such illumination at large angles does, however, create a complicated excitation volume at the interface with strong concentric side-lobes.

To achieve a TIRF excitation of submicrometer size, an element is required that works at diffraction-limited performance, even at very large illumination angles. On this account, we have recently introduced a parabolic mirror objective (PMO) that allows diffraction-limited high-aperture optics, as required in scanning confocal TIRF microscopy.[19,20] A cone of captured angles up to 80 deg can be used that enables the collection of surface-generated fluorescence with a high suppression of the background noise. As a consequence, the PMO optical elements are highly efficient tools for fluorescence biochemical applications at the water/glass interface.[21–24] By using the PMO in TIRF excitation geometry, one causes a probe depth of the order of $\sim\lambda/6$ at the glass/

Address all correspondence to Stefan Seeger, Institute of Physical Chemistry, University of Zurich, Winterthurerstrasse 190, Zurich CH-8057 Switzerland; Tel: +41 44 635 44 51; Fax: +41 44 635 68 13; E-mail: sseeger@pci.unizh.ch

1083-3668/2007/12(3)/034012/7/$25.00 © 2007 SPIE

water interface and consequently prevents the observation of fluorophores in solution.

Here, we present a different optical PMO configuration as an efficient fluorescence collection element at the interface and simultaneously in the solution. In contrast to high-angle excitation, the present optical geometry achieves its surface detection confinement by collecting the fluorescence at very high angles, exceeding the critical angle for total internal reflection at the water/glass interface. The excellent surface selectivity is obtained on the basis of the dipole emission profile near a dielectric interface.[25] Its angular distribution is a superposition of the traveling and evanescent waves. Propagating waves can be recorded in the far field at angles smaller than the critical angle for total internal reflection, and are sometimes called "allowed light." Consequently, dipoles located more than a decay length of the evanescent field from the interface will only participate with their traveling waves in the far-field detection. When the emitting dipole is in close proximity to a dielectric interface, the evanescent waves can couple to the medium with higher refractive index at angles above the critical angle. Such emission modes, called "forbidden light,"[26,27] can be converted into traveling waves via total internal reflection at the parabola/air interface, and subsequently recorded in the far field.[28,29] Hence, this is a practical substitute to TIRF geometry, which was referred to as the supercritical angle fluorescence (SAF) collection method.[30]

Using a subcritical angle excitation, the PMO objective described here has the ability to record both emission modes with two separated detection channels simultaneously. Thus, the system can provide information of the surface-bound and the unbound fraction of freely diffusing fluorophores at the same time. The following sections experimentally demonstrate the performance of the two parallel detection channels fluorescence microscope based on a resourceful parabolic mirror objective. Its optical resolution, imaging properties, and detection efficiency down to the single molecule level are discussed.

2 Supercritical Angle Fluorescence Microscope: Description and Performance

The theoretical description of the microscope using ray tracing calculations and a schematic presentation of how the system can be implemented were presented lengthily in a previous paper.[30] In this section, we describe the main parts of the microscope with attention for the major technical implementations in detail.

The experimental setup is shown in Fig. 1(a). A pulsed diode laser beam (635 nm, 50 ps, 80 MHz) coupled to a single-mode optical fiber and 1-mm waist collimated with an aspheric lens was used as excitation light. The laser beam is redirected with a dichroic mirror (XF2035, Omega Optical) and further enlarged by a factor of 6 using a beam expander. The expanded beam overfills the back aperture of the aspheric lens L4, which acts as an objective that focuses the excitation light at the surface of the sample. The aspheric lens objective was fixed on a hollow micrometer screw and embedded into the parabolic mirror.

With this mechanical approach, the aspheric lens relocates along the optical axis for fine adjustment in a range of a few micrometers. This aspheric lens is designed to focus a collimated light beam into a diffraction-limited spot through a glass window of 1.2 mm thickness. In this case, the window consists of a 1.05-mm-thick bridge-like top planar surface at the parabolic mirror center in addition to a 0.15-mm-thick microscope glass cover slip. These two parallel surfaces are connected with a very thin film of microscope oil (Merck immersion oil) to minimize the optical aberrations due to refractive index mismatch at the interfaces. The aspheric objective collects the fluorescence as in epifluorescence microscope geometries[31] in a range of angles between 0 and 24 deg (0.62 numerical aperture), which amounts to approximately 6% of the overall emitted fluorescence.

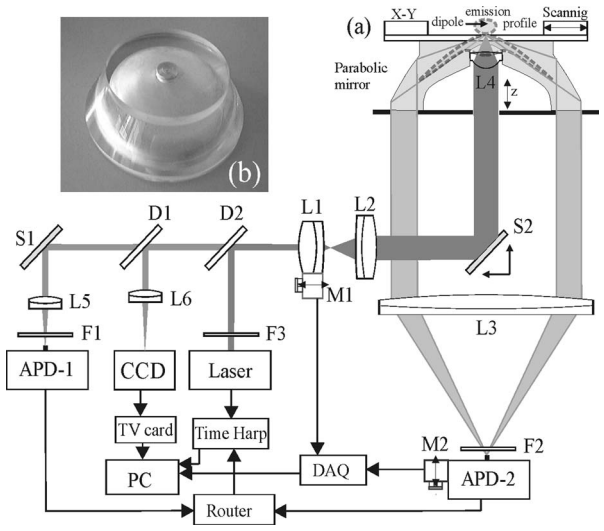

Fig. 1 (a) Schematic representation of the SAF microscope: L1 to L6 lenses, F1 to F3 fluorescence filters, M1 and M2 steppers, D1 and D2 dichroics, S1 and S2 mirrors, and APD-1(-2) avalanche photodiodes. The dashed lines illustrate the emission profile of the dipole near the dielectric interface. (b) Photograph of parabolic mirror.

It passes the dichroics D1 and D2 and is subsequently refocused onto the sensitive area of a photodiode (ASL channel, APD-1), (SPCM-AQR 13, Perkin-Elmer, Canada).

We used a PMO made from Zeonex with a focal length of 7.1 mm [Fig. 1(b)]. The outer diameter limits the minimum angle collection to 62 deg, which is above the critical angle of ~61 deg for the water/glass interface, whereas an opaque aperture beneath the PMO limits the angle collections under 75 deg. An antireflex layer was deposited on the underside face of the PMO to diminish the loss of the collected light. Approximately 34% of the overall fluorescence is emitted above the critical angle, but only ~2% above 75 deg.[26] Thus, the PMO collects most of the emitted fluorescence above the critical angle (~32%) and significantly suppresses the scattered light arising from angles beyond 75 deg. The light emitted into the lower half-space is transformed in a parallel beam through total internal reflection at the parabola/air interface. Subsequently, it is refocused by the 300-mm focal distance achromatic lens L3 onto a second avalanche photodiode (SAF channel, APD-2). A combination of bandpass and long-pass interference filters (Semrock, USA) was used in front of both detectors to reject the Rayleigh and Raman scattered light. The small diameter photosensitive area of the detectors acts as a confocal detection aperture.[32] The photon counts of the two

avalanche photodiodes were fed into a router (PRT 400, PicoQuant) and consequently recorded with a time-correlated single photon counting (TCSPC) card (TimeHarp 200) in a "time-tagged time-resolved" mode (TTTR).[33] As a result, the microscopic time (50-ps resolution) and the macroscopic time (100-ns resolution) of arriving photons are recorded and can be subsequently analyzed with respect to the lifetime dynamics or intensity trajectories of single molecules.[34] Scanning the sample was achieved by sliding the cover slip mounted on a metallic holder with a microscope stage (ScanIm 120×100, Märzhäuser, Germany) over the front face of the PMO. All optical components are mounted below the cover slip, leaving free access to the sample from above.

The capillary forces keep the vertical position of the glass cover slip constant (submicron range) for sizeable lateral movements. This is due to a significant contact area between the cover slip and the upper surface of the PMO (5 cm^2) by means of the microscope oil film. In this respect, scanning large areas ($\sim$1 cm^2) is possible without a dynamic focusing control of the objective lens as often needed in confocal microscopes.[33,35] The laser focus at the glass/air interface is obtained by moving the expander lens L1 along the optical axis with a motorized linear stage M1, whereas the distance between the beam expander lens L2, and the objective was kept fixed. The position and shape of the detected volume element for the ASL channel (APD-1 detector) are not affected by the optical adjustment for small variations in cover slip thicknesses. The image focus position of the objective lens in this optical geometry rests unaffected in the proper plane of the confocal detection, like in conventional epifluorescence microscopes.[35] Using the light back reflection from the cover slip air interface, a charge-coupled device (CCD) camera and a TV card are used to control the focus position at the sample surface.

A different approach is needed for the SAF channel (APD-2 detector). When the vertical position of the glass/air interface is shifted by different thicknesses of the cover slips, the SAF focused image moves along the optical axis of the achromatic lens L3. A second motorized linear stage M2 relocates the detector APD-2 to the SAF image focal point. Custom-written software drives the two motorized linear stages in a closed loop control, moving the expander lens L1 with 1 mm and the SAF detector with 0.18 mm, respectively, for every micron deviation of the cover slip from the standard thickness of 150 μm. The fluorescence detection efficiency of the system depends on the fraction of the emitted light in the range of captured angles and the transmission efficiency of other optical elements employed in the system. Hence, for the SAF channel, the detection efficiency is found to be 16%, while for the inner ASL channel, the overall detection efficiency amounts to approximately 2.5%.

3 Results and Discussions

The two fluorescence optical detection channels have detection volumes of completely different shapes along the optical axis. The ASL channel gives access to the light emission from deep inside the analyte solution ($\sim$2.5 μm), whereas the SAF channel acquires the emission of fluorophores located very close to the glass/water interface ($\sim$130 nm).[30] Therefore, two scanned images can be performed simultaneously, giving information from far- and near-field emission of the fluorophores. We used a low concentration aqueous solution of fluorescent beads (FluoroSphere, dark red, Molecular Probes) at pH 7.4 to experimentally investigate the imaging performance of the microscope. With a diameter of only 20 nm (3% of emission wavelength), the beads are stable point emitters to determine the instrumental point-spread function. Figures 2(a) and 2(b) shows scanning confocal intensity images of fluorescent beads in solution (20 μl) on a common glass cover slip, recorded with both channels. Scanning the surface was performed from top to bottom and from left to right with a spatial resolution of 156 nm per pixel. The scanned area is $\sim$78 $\times$78 μm with 1-ms intensity integration time. Figure 2(a) was recorded with the ASL channel and Fig. 2(b) with the SAF channel, respectively. Due to different detection volumes along the optical axis, different images of the same area recorded at the same time are shown. The ASL channel shows a

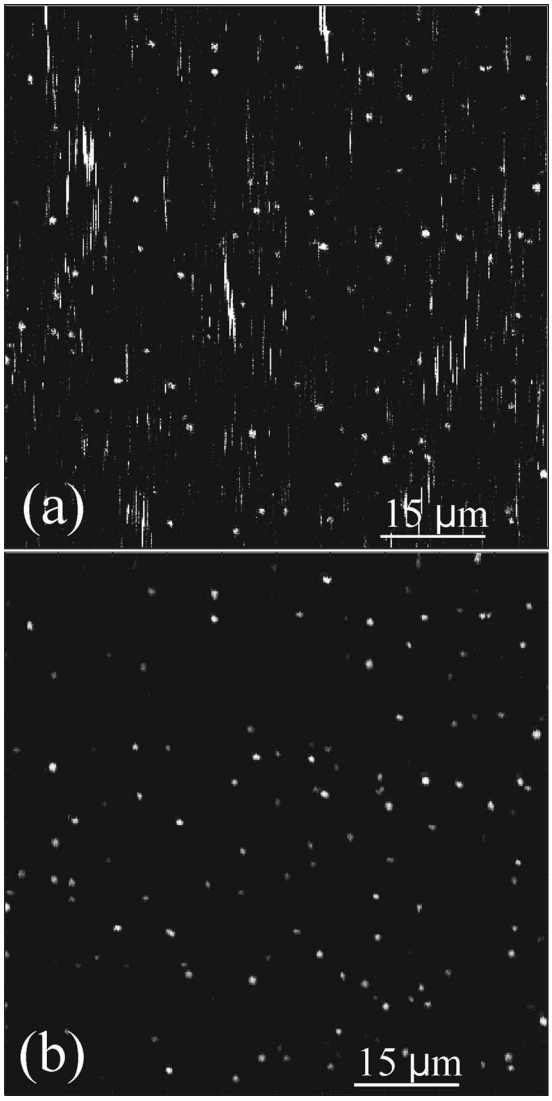

Fig. 2 Fluorescence intensity image (logarithmic scale) of beads in solution (78×78 μm): (a) ASL channel and (b) SAF channel. The surface scan was performed from top to bottom and from left to right with a resolution of 156 nm per pixel, and the photons were binned into 1-ms time bins.

fluorescence image of beads adsorbed at the surface of the cover slip (round spots), and bright vertical lines along the scanned direction attributed to freely diffusing fluorophores into the objective detection volume. Some longer and brighter lines are most likely due to bead aggregates diffusing slower inside the larger detection volume created by the aspheric objective. In comparison, the SAF channel (i.e., supercritical angle detection), shows only the image of the beads adsorbed on the glass surface. A signal-to-background ratio (S/B) of up to 55 was measured for the SAF channel, while a value of 10 was obtained for the ASL channel, respectively. Thus the S/B ratio measured is in line with the calculated factor of 5 between the two detection channels.[30] The background for the SAF channel arises mainly from the surface Raman scattered photons passing the emission filter. A significant advantage of the SAF-PMO objective over objective-type TIRF is that in the former geometry, the SAF emission is totally separated from the excitation light path. Consequently, the surface selectivity arises entirely in the emission path. Therefore, there is no need to filter out the excitation light with high optical density emission or dichroic filters. The missing dichroic in the SAF channel is advantageous when a FRET filter, multicolor dichroics (multiplexing) mirrors, or polarization prisms are desired. The intensity difference between the two images is mainly due to a much higher light collection efficiency of the parabolic mirror, which can be explained by the behavior of the dipole emission profile at the dielectric interface.[25,26] Therefore, the surface-bound fluorophores can be detected with a high signal-to-background ratio without interferences of fluorescence from diffusing molecules in the bulk solution. The photons detected with the SAF channel originate entirely from the near-field emission of the fluorophores located within a distance from the interface in the order of a third of the emission wavelength. All fluorophores positioned at longer distances from the dielectric interface contribute with their emission to under the critical angle and in this way, partially detected with the inner aspheric channel.

The lateral resolution of the microscope is limited by the size of the laser focus at the glass/water interface and is identical for both detection channels. Thus, the optical focusing performance of the aspheric lens objective is the limiting factor for the lateral resolution, assuming that its back aperture plane is slightly overfilled with a well-collimated Gaussian beam. Figure 3 shows the linear cross section of an imaged bead, immobilized at the glass/water interface. A Gaussian fit gives a full-width at half-maximum (FWHM) of 510±5 nm in the horizontal plane for the ASL inner channel [Fig. 3(a)], and 515±5 nm for the SAF channel [Fig. 3(b)], respectively. The measured FWHM values are slightly higher than those calculated for confocal microscopy, which amounts to 470 nm, $(0.5\lambda/\sqrt{2}\cdot NA)$.[36] This can be explained by taking into consideration that the aspheric lens is designed to perform diffraction-limited focusing for a higher wavelength than was used in the present experiment. Additionally, the lens was engineered to focus the light through a glass window with a smaller refractive index than that of the cover slips used. Small aberrations in the additional optic elements also alter the spatial intensity distribution and thus give a focus spot size slightly larger than the diffraction limit.

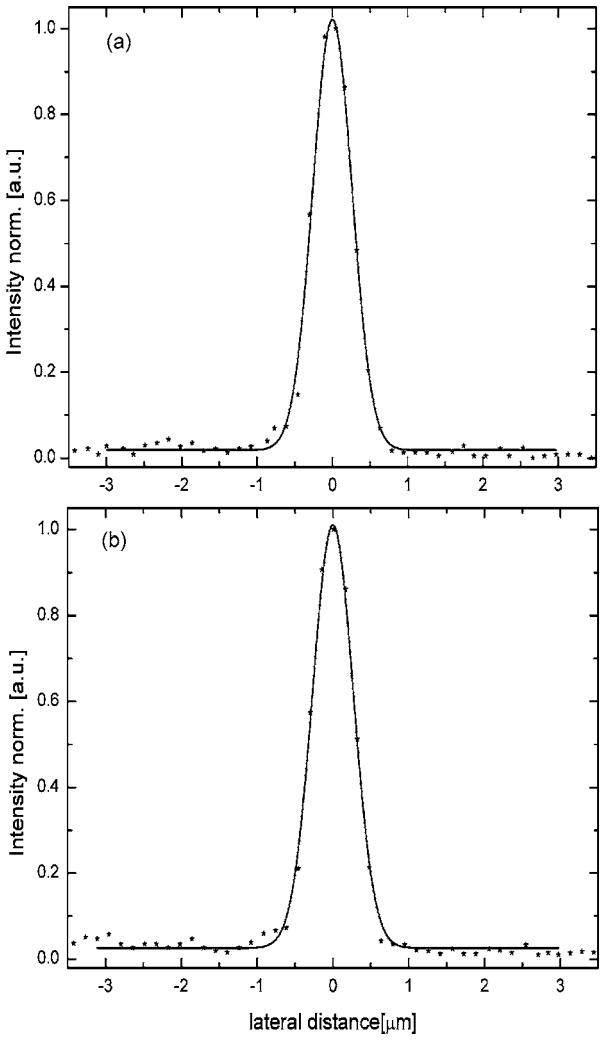

Fig. 3 Optical resolution for both detection channels: (a) ASL channel and (b) SAF channel. The spatial resolution is 156 nm per pixel.

The $1/e^2$ intensity dropoff in the axial direction was calculated for the ASL channel to be $\sim 2.5\ \mu$m, and for the SAF channel $\sim$130 nm, correspondingly. Compared with conventional objective-type TIRF systems, the described microscope generates a significantly smaller excitation area at the interface.[19,20,37]

Clearly, the excitation area for the PMO objective is much smaller than the edge illumination of objective-type TIRF systems, which can be up to few microns large. In the case of annular illumination of objectives, the focus spot at the interface can be smaller than the edge excitation, but the side lobes of the excitation profile rise rapidly (up to 35% of the central illumination) with the increasing excitation angles.[17,20] Such excitation above the critical angle can be obtained by using an opaque disk in front of the expanded incident light, creating a donut shape for the excitation beam. Likewise, up to 90% of the incident energy is blocked in this geometry illumination. Therefore, a low angle excitation like in the present setup is more advantageous over objective-type TIRF geometries that involve high-angle illumination and hence are prone to spherical aberrations and other technical difficulties.

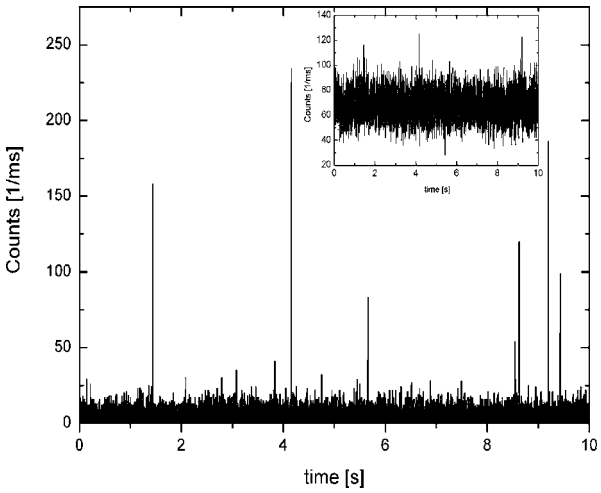

Fig. 4 Fluorescence bursts for single Cy5 molecules (1-nM concentration) binding nonspecifically on a hydrophilic glass cover slip (SAF channel). The inset plot shows the time trace of the ASL channel in the same conditions.

To determine the sensitivity of the PMO objective in the SAF geometry for detecting single molecules, a red dye as a test sample has been used. Figure 4 shows time traces for single Cy5 molecules (1-nM concentration) undergoing adsorption and desorption on hydrophilic glass cover slides.[32] Data collected in this manner allow the observation of characteristic photon bursts of single molecules diffusing through an open probe volume or of those nonspecifically attached on the glass surface. Due to the small SAF detection volume confined at the interface, the short bursts shown in Fig. 4 are most likely from single Cy5 molecules undergoing reversible adsorption on the glass surface. Because the molecules cross the detection volume or adsorb/desorb onto the surface at random times, the probability of detecting molecules at any given time follows the well-known Poisson distribution. The average number of Cy5 molecules within the SAF probe volume and 1-nM concentration is only 0.02. As a consequence, the detection volume is most of the time unoccupied ($\sim$98%), and contains one and two molecules $\sim$2% and $\sim$0.02% of the time, respectively. An S/B ratio of 40 was obtained for the highest peak in Fig. 4 at the given background of 6 counts per 1 ms time binning and a laser power of 40 μW. The inset of Fig. 4 shows the time traces of the same Cy5 sample recorded with the confocal ASL channel (APD-1). In this case, a count rate uniformly distributed around 70 cpms was recorded. Due to a larger detection distance along the optical axis for the ASL channel, more than one Cy5 molecule may be present in the detection volume at nanomolar concentration in water. However, fluorescence bursts of single Cy5 molecules diffusing into the detection volume of the inner ASL channel with an $S/B \approx 2$ are detected (see Fig. 4, inset).

We have shown before that an aspheric lens objective with an NA of 0.62 (i.e., only 6% of all emitted fluorescence is collected) can record fluorescence bursts of single Cy5 molecules in aqueous solutions down to picomolar concentrations.[35] In the case of an open sample solution, the fluorophores move in and out of the detection volume due to their Brownian motion. Hence, most analyte molecules will

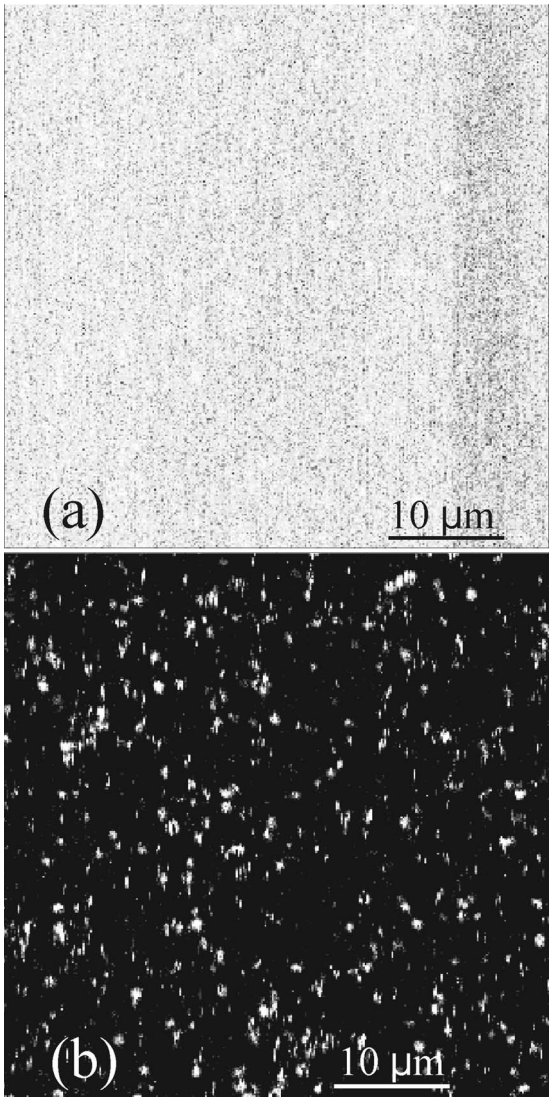

Fig. 5 Fluorescence images of single Cy5 molecule 1 nM adsorbed on a glass surface (78×78 μm) recorded via: (a) ASL channel and (b) SAF channel (logarithmic intensity scale).

cross the detection volume at the edge, leading to small burst sizes. In other words, only molecules passing through the maximum of the detection volume may give rise to detectable bursts in the ASL channel. Scanning dual microscopy images obtained for single Cy5 molecules adsorbed on the cover slide are shown in Fig. 5. An aqueous solution of Cy5 molecules (1-nM concentration, 20 μL) was dropped on the surface of a glass cover slip and a scanned image with an integration time of 1 ms per pixel was performed 5 min later. A certain number of Cy5 molecules adsorb on the glass surface and shows diffraction-limited spots with count rates up to 200 kHz [Fig. 5(b)]. Signal-to-background ratios of up to 20 with a background count rate of $\sim$10 kHz were obtained for the most intense pixels. Some pixels appear dark within the bright spots, specifically for single molecules that undergo blinking or single step photobleaching, which is a clear criterion for single-chromophore systems.[38] Moreover, image spots at different positions have different intensities due to different mo-

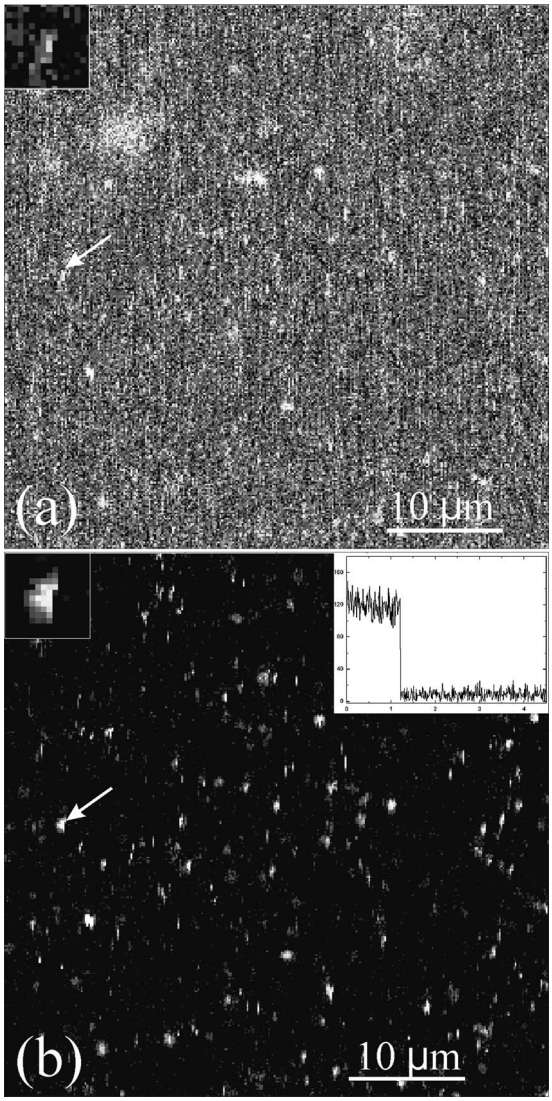

Fig. 6 Fluorescence images of single Cy5 molecule (0.5 nM) adsorbed on a glass surface (47×47 μm) recorded via: (a) ASL channel and (b) SAF channel, respectively (logarithmic intensity scale). The arrows in the figures point to the image of a single molecule undergoing one step photobleaching as depicted in the top-left insets. The data are binned into 1-ms time bins.

lecular orientations and microenvironments. The freely diffusing molecules do not affect the scanned image in the SAF channel, as their fluorescent contribution to the total intensity is merely at the background level. On the contrary, the image recorded with the ASL channel was saturated by the presence of diffusing molecules in a larger detection volume created by the aspheric objective lens [Fig. 5(a)].

Only a few bright spots can be seen, which are heavily overwhelmed by the large fluorescence of diffusing fluorophores in the detection volume. In this respect, Fig. 6 shows a scan image recorded in the same conditions but for a concentration of 0.5 nM of Cy5 in water (47×47 μm). At this concentration, fewer molecules are adsorbed on the glass surface during the scanning time.

Decreasing the concentration results in a corresponding reduction in the frequency of adsorbed molecules, but the average characteristic parameters such as size of the bright spots and their amplitude remain constant. This indicates that single molecule events are detected with both channels. Figure 6(a) shows an image recorded with the ASL channel and Fig. 6(b) with the SAF channel, respectively.

As a result of the low numerical aperture of the aspheric lens in the ASL channel, the achieved signal-to-background ratio is weaker than with high aperture microscope objectives typically used in single molecule experiments. However, some of the brightest spots attributed to the single molecules adsorbed on the surface are present in both images. The arrows in both figures point to single molecule images undergoing one step photobleaching during the scan.[39] After the scan, a few bright spots were constantly illuminated until irreversible single-step photodestruction occurred. The inset (top right) of Fig. 6(b) shows the count time trace recorded for one image bright spot, which resembled one-step bleaching behavior of a single Cy5 molecule.

4 Conclusion

We describe the design and construction of a new confocal fluorescence microscope as an alternative to the widely used objective-type TIRF systems. The supercritical angle detection technique is advantageous over epifluorescence microscopes when it is applied to the detection in complex environments where one encounters background fluorophores at distances greater than the evanescent depth. The possibility to illuminate the sample at low surface angles offers a simultaneous detection in the analyte solution. Such an excitation approach is technically easier and gives an improvement over objective-type TIRF, which requires very high angles for excitation. In practice for example, with a 1.4 numerical aperture objective, only 2.8% of its aperture can be used for TIRF illumination. Hence, correctly coupling the laser into the objective back focal plane is technically challenging.[40] On the other hand, high index glass cover slips and special microscope oil are required for the 1.65 numerical aperture objectives.[40,41] The two-channel microscope described uses only disposables currently used in fluorescence microscopy, like common cover slips and regular microscope oil. Furthermore, it is difficult to produce an excitation spot of submicron dimensions using various TIRF methods, whereas with the geometry presented, diffraction-limited resolution is straightforward. So far, we have only used a commercially available aspheric lens with a numerical aperture of 0.62 for sample illumination. Consequently, the focusing performance of the aspheric lens is the limiting factor for the optical resolution of the microscope and the detection efficiency of the inner channel. A numerical aperture of the aspheric lens objective higher than 1.0 will give a better volume restriction ($\sim$1 fl or less), optical resolution, and a superior collection efficiency for the inner channel, which is imperative in the case of single molecule detection. Currently, we are exploring a smaller geometry of the PMO explained that will fit in any turret of normal epifluorescence microscopes. The implementation to any epifluorescence geometries will be straightforward without any modification in the frame of commercial microscopes. The only technical approach needed is the separation of the two detection channels after the dichroic cube. This modification can be performed at the exit-side fluorescence ports of any

upright microscope by using a 6-mm-diam mirror fixed on the center of an emission filter or a glass window, for example. Such small mirrors with an elliptical top surface for 90-deg reflection are already commercially available. Thus, two perpendicular emission paths outside the microscope main frame can be obtained easily. Detecting the volume and surface generated fluorescence simultaneously can be of great benefit in cell biology, for example, when one encounters fluorophores in the membrane and deeper inside the cell. An excellent signal-to-background ratio at moderate illumination intensity, high resolution imaging, radical reduction of the detection volume along the optical axis, and easy handling and stability, make the two-channel fluorescence microscope a nice technique for surface fluorescence measurements down to the single molecule level.

Acknowledgment

The authors wish to acknowledge the support of the Swiss National Science Foundation.

References

1. X. S. Xie and J. K. Trautman, "Optical studies of single molecules at room temperature," *Annu. Rev. Phys. Chem.* **49**, 441–489 (1998).
2. S. Weiss, "Fluorescence spectroscopy of single biomolecules," *Science* **283**, 1676–1682 (1999).
3. S. T. Hess, S. Huang, A. A. Heikal, and W. W. Webb, "Biological and chemical applications of fluorescence correlation spectroscopy: A review," *Biochemistry* **41**(3), 697–705 (2002).
4. C. R. Taittt, G. P. Anderson, and F. S. Ligler, "Evanescent wave fluorescence biosensors," *Biosens. Bioelectron.* **20**(12), 2470–2487 (2005).
5. G. Stengel and W. Knoll, "Surface plasmon field enhanced fluorescence spectroscopy studies of primer extension reaction," *Nucleic Acids Res.* **33**(7), 1–10 (2005).
6. D. Axelrod, "Cell-substrate contacts illuminated by total internal reflection fluorescence," *J. Cell Biol.* **89**, 141–145 (1981).
7. X. H. Xu and E. S. Yeung, "Direct measurement of single-molecule diffusion and photodecomposition in free solution," *Science* **275**, 1106–1109 (1997).
8. G. I. Mashanov, D. Tacon, A. E. Knight, M. Peckham, and J. E. Molly, "Visualizing single molecule inside living cells using total internal reflection fluorescence microscopy," *Methods* **29**, 142–152 (2003).
9. T. Wazawa, Y. Ishi, T. Funatsu, and T. Yanagida, "Spectral fluctuation of a single fluorophore conjugated to a protein molecule," *Biophys. J.* **78**, 1561–1569 (2000).
10. W. P. Ambrose, P. M. Goodwin, and J. P. Nolan, "Single-molecule detection with total internal reflection excitation: comparing signal-to-background and total signal in different geometries," *Cytometry* **36**, 224–231 (1999).
11. M. F. Paige, E. J. Bjerneld, and W. E. Moerner, "A comparison of through-the-objective total internal reflection microscopy and epifluorescence microscopy for single-molecule fluorescence imaging," *Single Mol.* **2**(3), 191–201 (2001).
12. K. Hassler, T. Anhut, R. Rigler, M. Gösch, and T. Lasser, "High count rates with total internal reflection fluorescence correlation spectroscopy," *Biophys. J.* **88**(1), L01–L03 (2005).
13. M. Oheim, D. Loerke, R. H. Chow, and W. Stühmer, "Evanescent-wave microscopy: a new tool to gain insight into the control of transmitter release," *Philos. Trans. R. Soc. London, Ser. B* **354**, 307–318 (1999).
14. A. D. Stout and D. Axelrod, "Evanescent field excitation of fluorescence by epiillumination microscopy," *Appl. Opt.* **28**, 5237–5242 (1989).
15. D. Axelrod, "Total internal reflection fluorescence microscopy in cell biology," *Traffic (Oxford, U. K.)* **2**, 764–774 (2001).
16. D. Toomre and D. J. Manstein, "Lighting up the cell surface with evanescent wave microscopy," *Trends Cell Biol.* **11**(7), 298–303 (2001).
17. T. P. Burghardt, K. Ajtai, and J. Borejdo, "In situ single molecule imaging with attoliter detection using objective total internal reflection confocal microscopy," *Biochemistry* **45**, 4058–4068 (2006).
18. B. Sick, B. Hecht, and L. Novotny, "Orientational imaging of single molecules by annular illumination," *Phys. Rev. Lett.* **85**(21), 4482–4485 (2000).
19. T. Ruckstuhl and S. Seeger, "Attoliter detection volumes by confocal total-internal-reflection fluorescence microscopy," *Appl. Opt.* **29**, 569–571 (2004).
20. T. Ruckstuhl and S. Seeger, "Confocal total-internal-reflection fluorescence microscopy with a high-aperture parabolic mirror lens," *Appl. Opt.* **42**, 3277–3283 (2003).
21. A. Krieg, S. Laib, T. Ruckstuhl, and S. Seeger, "Real-time detection of nucleotide incorporation during complementary DNA strand synthesis," *ChemBioChem* **4**, 589–592 (2003).
22. A. Krieg, S. Laib, T. Ruckstuhl, and S. Seeger, "Fast detection of single nucleotide polymorphisms (SNPs) by primer elongation with monitoring of supercritical-angle fluorescence," *ChemBioChem* **5**, 1680–1685 (2004).
23. A. Krieg, T. Ruckstuhl, S. Laib, and S. Seeger, "Real-time detection of polymerase activity using supercritical angle fluorescence," *J. Fluoresc.* **14**, 75–78 (2004).
24. T. Ruckstuhl and A. Krieg, "Microscope objective for large-angle fluorescence used for rapid detection of single nucleotide polymorphisms in DNA hybridization," *Anal. Chem.* **77**, 2656–2661 (2005).
25. J. Enderlein, T. Ruckstuhl, and S. Seeger, "Highly efficient optical detection of surface-generated fluorescence," *Appl. Opt.* **38**, 724–732 (1999).
26. T. Ruckstuhl, J. Enderlein, S. Jung, and S. Seeger, "Forbidden light detection from single molecules," *Anal. Chem.* **72**, 2117–2123 (2000).
27. B. Hecht, "Forbidden light scanning near-field optical microscopy," Doctoral Thesis, Univ. Basel, Switzerland (1996).
28. H. F. Arnoldus and J. T. Foley, "Spatial separation of the traveling and evanescent parts of dipole radiation," *Opt. Lett.* **28**(15), 1299–1301 (2003).
29. H. F. Arnoldus and J. T. Foley, "Transmission of dipole radiation through interfaces and the phenomenon of anti-critical angles," *J. Opt. Soc. Am. A* **21**(6), 1109–1117 (2004).
30. T. Ruckstuhl and D. Verdes, "Supercritical angle fluorescence (SAF) microscopy," *Opt. Express* **12**(18), 4246–4254 (2004).
31. R. H. Webb, "Confocal optical microscopy," *Rep. Prog. Phys.* **59**, 427–471 (1996).
32. W. E. Moerner and D. P. Fromm, "Methods of single-molecule fluorescence spectroscopy and microscopy," *Rev. Sci. Instrum.* **74**(8), 3597–3619 (2003).
33. M. Böhmer, F. Pampaloni, M. Wahl, H. J. Rahn, R. Erdmann, and J. Enderlein, "Time-resolved confocal scanning device for ultrasensitive fluorescence detection," *Rev. Sci. Instrum.* **72**(11), 4145–4152 (2001).
34. C. Eggeling, A. Volkmer, and C. A. M. Seidel, "Molecular photobleaching kinetics of Rhodamine 6G by one- and two-photon induced confocal fluorescence microscopy," *ChemBioChem* **6**, 791–804 (2005).
35. T. Ruckstuhl, A. Walser, D. Verdes, and S. Seeger, "Confocal reader for biochip screening and fluorescence microscopy," *Biosens. Bioelectron.* **20**, 1872–1877 (2005).
36. G. Cox and C. J. R. Sheppard, "Practical limits of resolution in confocal and non-linear microscopy," *Microsc. Res. Tech.* **63**, 18–22 (2004).
37. K. Hassler, M. Leutenegger, P. Rigler, R. Rao, R. Rigler, M. Gösch, and T. Lasser, "Total internal reflection fluorescence correlation spectroscopy (TIR-FCS) with low background and high count-rate per molecule," *Opt. Express* **13**(19), 7415–7423 (2005).
38. J. J. Macklin, J. K. Trautman, T. D. Harris, and L. E. Brus, "Imaging and time-resolved spectroscopy of single molecules at an interface," *Science* **272**, 255–258 (1996).
39. Z. Huang, D. Ji, and A. Xia, "Fluorescence intensity and lifetime fluctuations of single Cy5 immobilized on the glass surface," *Colloids Surf., A* **257–258**, 203–209 (2005).
40. D. Axelrod, "Selective imaging of surface fluorescence with very high aperture microscope objective," *J. Biomed. Opt.* **6**(1), 6–13 (2001).
41. Y. Kawano and R. G. Enders, *Total Internal Reflection Fluorescence Microscopy* Application Note, Olympus America Inc., (1999).